J Therm Anal Calorim (2009) 97:157–161
DOI 10.1007/s10973-009-0248-4

Carbothermal reduction of the YSZ–NiO solid oxide fuel cell anode precursor by carbon-based materials

E. Arico · F. Tabuti · F. C. Fonseca · D. Z. de Florio · A. S. Ferlauto

ICTAC2008 Conference

Abstract The thermal behavior of the yttria-stabilized zirconia (YSZ) and nickel oxide (YSZ–NiO) composite mixtures with the addition of graphite, multiwall carbon nanotubes and functionalized multiwall carbon nanotubes was studied. The YSZ–NiO composite is the precursor of the YSZ–Ni anode of solid oxide fuel cells. The anode exhibits a porous structure, which is usually obtained by the addition of carbon containing pore formers. Thermal analysis and X-ray diffraction evidenced that the properties of carbonaceous materials (C) and atmosphere have a strong influence on the thermal evolution of the reactions taking place upon heating the anode precursor. The dependence of both the carbon content and the chemical nature of the ceramic matrix on the thermal behavior of the composite were investigated. The discussed results evidenced important features for optimized processing of the anode.

Keywords Carbothermal reduction · Carbon nanotube · Solid oxide fuel cell · YSZ–Ni anode

Introduction

Fuel cells are energy conversion devices that produce electricity and heat direct from the reaction of a fuel and an oxidant [1–4]. They are classified according to the characteristics of the electrolyte, fuel, and the operation temperature. Among the different types of fuel cells the solid oxide fuel cell (SOFC) is the one under active development that presents several distinct advantages promoted by both the all-solid state components and the high operation temperature in the 700–1000 °C range. Such high temperatures contribute to the absence of noble metals as catalysts and the ability of operation on various fuels. The SOFC consist basically of two porous electrodes (the anode and the cathode) separated by a dense oxide ion conductor (the electrolyte). The ceramic components that have been most used in the SOFC are the solid electrolyte yttria-stabilized zirconia (YSZ); the YSZ–Ni cermet anode, and the La-doped manganite cathode [1–4].

The anode is the fuel electrode and is directly related to the SOFC performance; it must be stable in the reducing environment of the fuel, electrically conductive and must have sufficient porosity to allow the transport of both the fuel and the reaction products of fuel oxidation. In order to maintain the porous structure of the nickel over long periods at high temperatures, nickel is often dispersed in an YSZ matrix. The anode cermet is commonly prepared from nickel (II) oxide powder and YSZ. Nickel is formed by the reduction of nickel oxide during fuel cell operation. The oxygen release during NiO reduction leads to some porosity; however, additional porosity is necessary in order to have an effective mass transport across the anode, and it is usually attained by the addition of pore formers to the YSZ–NiO precursor.

The present study is related to the engineering of the porous structure of the anode by using different high surface area carbonaceous (C) pore formers, such as carbon nanotubes (CNT), functionalized carbon nanotubes (f-CNT), and graphite (G). The main objective of the present study

E. Arico (✉) · F. Tabuti · F. C. Fonseca
CCCH—IPEN-CNEN/SP, Av. Prof. Lineu Prestes 2242, São Paulo, SP, Brazil
e-mail: emarico@ipen.br

F. Tabuti · D. Z. de Florio
CECS—UFABC, R. Santa Adélia 166, Santo André, SP, Brazil

A. S. Ferlauto
Departamento de Física, UFMG, Belo Horizonte, MG, Brazil

is to investigate the release of carbon and oxygen during the sintering process of the ceramics by systematic thermogravimetric (TG) analyses of the precursor powder YSZ–NiO + C.

Experimental

A modified liquid mixture technique was used to prepare the YSZ–NiO precursor corresponding to the YSZ–Ni cermet with 45 vol.% Ni after NiO reduction [2]. The preparation involves the evaporation of a dispersion of yttria-stabilized zirconia (Tosoh) in a nickel (II) acetate tetrahydrate (Carlo Erba) and ethanol solution with the relative composition of 39 mass% YSZ and 61 mass% NiO (YSZ–61NiO), which is equivalent to ~59 vol.% of NiO. The liquid mixture was held in ultrasonic bath for 1 h and heated on a hot plate under vigorous stirring to evaporate the alcohol. The prepared powder was dried at 80 °C and calcined at 450 °C in air for 5 h. The carbonaceous species CNT, f-CNT, and G were mixed to YSZ–NiO composite with relative weight fractions of 10 and 20 mass%.

Multiwall carbon nanotubes were produced by chemical vapor deposition by using ethylene and ferrocene as carbon and catalyst sources, respectively. The functionalized carbon nanotubes were obtained by refluxing the as-grown CNT in nitric acid. Further details of CNT production are found elsewhere [5].

Thermogravimetric (TG) analyses were performed with a Setaram TG/DTA Labsys™ using alumina crucibles. Before each TG measurement the system was heated from room temperature to 30 °C and equilibrated for 10 min. The curves were registered at a heating rate of 10 °C/min in the 30–1350 °C temperature range; and under different gases [argon (99,9999%), synthetic air, and a gas mixture of 96% Ar/4% H_2] at 40 mL/min flow rate. Analysis under the reducing gas mixture were performed up to 900 °C and some of them were isothermally held at the maximum temperature up to 1 h in order to assure the total reduction of NiO. All curves were subtracted from the characteristic background of the apparatus by performing TG measurements with blank crucibles under the same experimental conditions.

X-ray diffraction (XRD, RIGAKU Miniflex) data of TG residues and as-prepared powders were collected using CuKα radiation in the $22.5^\circ \leq 2\theta \leq 55^\circ$ range, scan rate 0.05°, and 2 s counting time.

Results and discussion

The TG curves of the mixtures YSZ–NiO + 10 mass% C with C being graphite (G), multiwall carbon nanotubes (CNT) and functionalized multiwall carbon nanotube (f-CNT) performed in both synthetic air and argon dynamic atmosphere are presented in Fig. 1.

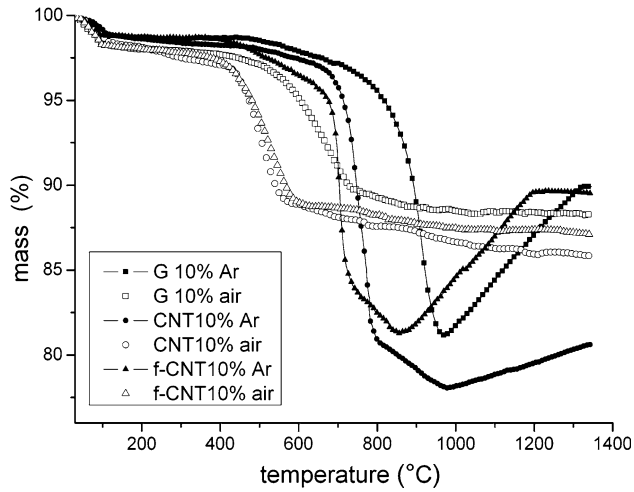

Fig. 1 Thermogravimetric curves of the YSZ–NiO + 10 mass% carbon in air and argon. *G* graphite, *CNT* carbon nanotubes, *f-CNT* functionalized carbon nanotubes

In all TG curves a small mass loss of ~2% takes place at ~100 °C, which was attributed to water release. In synthetic air (Fig. 1) only the oxidation of C species occurred and both the CNT and f-CNT have similar mass loss onset at ~350 °C while the oxidation of graphite started at higher temperatures (~400 °C). The lower oxidation temperature of the nanotubes can be attributed to the curvature effect and/or defects in nanotube walls, which increase the local reactivity [6, 7]. For all carbon-based materials investigated, the results of the TG analyses in synthetic air resulted in total mass loss consistent with the nominal carbon content (10 mass%) suggesting that most of the added carbon is released around ~800 °C. Mass losses slightly higher than the theoretical value (10%). This means that the organic matter could not completely eliminate during the calcination of the YSZ–NiO precursor. The DTG curves (here are not presented) indicate that the maximum oxidation rate of the carbon pore formers occurred at 690, 520 and 500 °C for G, CNT, and f-CNT, respectively. No reduction of NiO was detected in the TG experiments performed in synthetic air.

On the other hand, the TG curves recorded under Ar flow exhibit different features. The onsets of mass loss are shifted to higher temperatures and were found to be dependent on the type of carbon (CNT, f-CNT, or G), being the value correspondent to f-CNT the lowest one (~600 °C). The theoretical values of the total mass loss in the (YSZ–61NiO) + 10 mass% C mixtures is 23%, being 10% due to C oxidation and 13% due to oxygen release of the NiO reduction. By increasing the temperature, resulted in rapid mass losses that reached maximum values of ~19% for both

f-CNT and G, occurring at ~860 °C and ~970 °C, respectively. In the case of CNT, the maximum mass loss at 970 °C is ~22%, a value equivalent to the theoretical one (23%). It is important to note that both CNT and f-CNT exhibit two mass loss steps with different slopes. The faster one, occurring at lower temperatures, has mass loss of ~13% for f-CNT at 730 °C and ~16% at 780 °C for CNT. Such values may be associated with the theoretical value for the oxygen release during NiO reduction (13%), indicating that the carbothermal reduction of NiO was completed. The slower mass loss step at higher temperature is probably due to either the oxidation of excess C and/or with a competing oxidation of C and reoxidation of Ni. Further heating up to 1350 °C resulted in mass gain of ~8% that was attributed to nickel reoxidation due to the presence of residual oxygen in the TG furnace. Both f-CNT and G have similar rates of Ni oxidation that stabilized at high temperatures, while CNT exhibited an incomplete reaction with slower rate up to 1350 °C.

In order to gain further information concerning the reactions taking place during the thermal treatments, residues of selected TG measurements were analyzed by X-ray diffraction (XRD). Figure 2 depicts the XRD patterns of YSZ–NiO + 10 mass% G, heated up to 950 °C and 900 °C in argon and reducing atmosphere, respectively; and of YSZ–NiO + 10 mass% f-CNT after heating up to 1350 °C in both argon and synthetic air. The pattern for the YSZ–NiO + 10 mass% G residue at 950 °C (Ar) exhibits small peaks related to both graphite at $2\theta^\circ = 26.5$ and NiO. In addition, intense peaks associated with nickel are observed at $2\theta^\circ = 44.5$ and 54.8. Such a result confirms that under inert atmosphere the mass loss is associated with the carbothermal reduction of Ni. The XRD pattern of the residue of the sample with G addition heated under reducing conditions up to 900 °C shows no evidence of NiO and some G remaining, suggesting that all NiO was reduced but an excess of G is still present. The residues of YSZ–NiO + 10 mass% f-CNT at 1350 °C have identical XRD patterns, regardless the flowing atmosphere during TG experiments. The main diffraction peaks belonging to the cubic phase of both YSZ ($2\theta^\circ = 29.9$, 34.8, and 50.2) and NiO ($2\theta^\circ = 26.5$, 37.5, and 43.3) were indexed. The absence of diffraction peaks corresponding to nickel indicates total reoxidation of Ni at high temperature under both argon and air flow. In Fig. 2 it is also shown the XRD pattern of the as-prepared YSZ–NiO composite that exhibits low intensity peaks corresponding to nickel. Such a small fraction of Ni is formed during the calcination step at 450 °C due to the release of carbon monoxide from the decomposition of the acetate precursor. The initial fraction of the metallic phase in the as-prepared composite may be responsible for small deviations of the mass loss values found in the TG analyses.

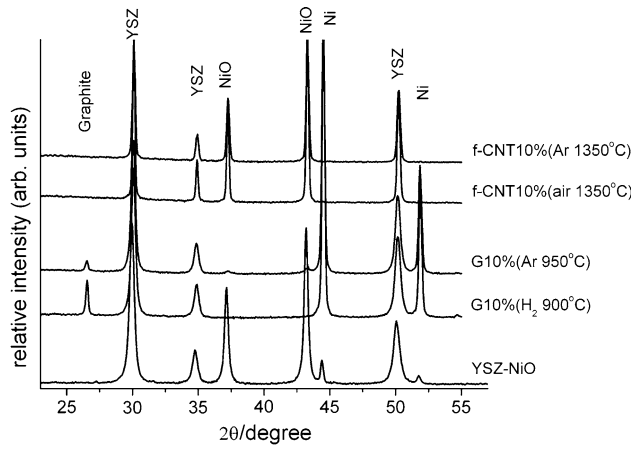

Fig. 2 X-ray diffraction patterns of as-prepared YSZ–NiO and TG residues of analyses at 1350 °C for YSZ–NiO + 10 mass% f-CNT (in air and Ar), YSZ–NiO + 10 mass% G (in Ar at 950 °C and in Ar/H_2 at 900 °C)

The influence of the carbon content on the reactions in argon was investigated in samples with the addition of 20 mass% C (C = G, CNT, and f-CNT) and the results are displayed in Fig. 3. From the TG curves it is observed that the mass loss onsets were not significantly changed with increasing C content (Fig. 1), and two mass loss steps with different slopes are shown. The TG data, displayed in Fig. 3, indicate that the curves for f-CNT, CNT, and G are similar to the ones shown in Fig. 1 up to the maximum temperature of the first mass loss step occurring at ~710, 780, and 870 °C, respectively. In addition, the estimated mass losses of the first step are compatible with the one expected for the NiO reduction in this mixture (10.4%). Further increasing the temperature, leads to the second mass loss step, which was considerably more affected by

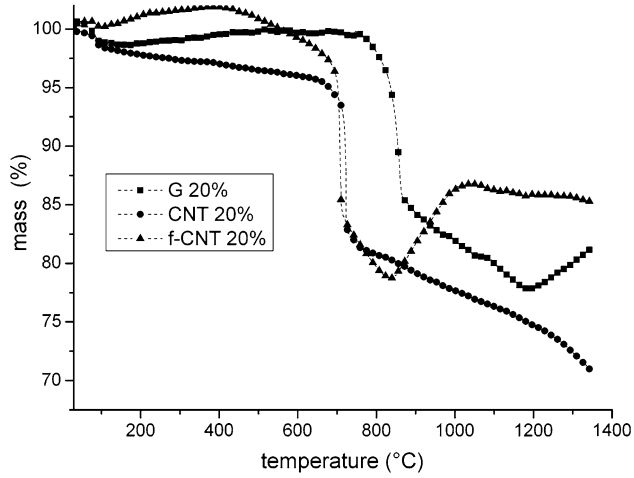

Fig. 3 Thermogravimetric curves for the YSZ–NiO + 20 mass% carbon in argon. *G* graphite, *CNT* carbon nanotubes, *f-CNT* functionalized carbon nanotubes

the increased C content (Fig. 1). The second mass loss step, preceding the mass gain at higher temperature, takes place over a wider temperature range in comparison to samples with lower C content, indicating that such step is related to the oxidation of excess C. Maximum mass loss for f-CNT and G samples were found to be ~78% at 840 and 1190 °C, respectively; and for the CNT sample, the second mass loss extends up to the maximum measuring temperature, reaching ~30%, a value close to the theoretical one for the total release of C and NiO reduction (30.4%). The distinct behavior of CNT, as compared to the other carbon based materials observed in Figs. 1 and 3 is not yet clearly understood. It is likely to be related either to the higher reactivity of the f-CNT, which favors the oxidation reaction of nanotubes, and/or to the impurity content of CNT samples, which have some residue of the catalyst, mostly Fe.

The total content of the nickel in the YSZ–NiO composite and the reaction mechanism for the specimens YSZ–NiO + 10 mass% G and YSZ–NiO + 10 mass% f-CNT were investigated by TG analyses under reducing atmosphere (96%Ar/4%H_2) up to 900 °C, as shown in Fig. 4.

The mass loss of the YSZ–NiO composite is complete at ~660 °C and corresponds to ~11%, a value close to the theoretical one (13%) for the NiO reduction. On the other hand, the TG curve under reducing atmosphere of the YSZ–NiO + 10 mass% G exhibited the first thermal decomposition step up to ~820 °C, with a mass loss of ~11% that could be attributed to the NiO reduction; followed by an incomplete second step. The combined results of TG and XRD of this sample residue (Fig. 2), indicate that the predominant mechanisms of the first and second mass loss steps are the reduction of NiO and C oxidation, respectively. For the sample YSZ–NiO + 10 mass% f-CNT a total mass loss of ~24 mass% was measured at ~900 °C, consistent with the total reduction of NiO and oxidation of f-CNT. However, to ensure the totality of the reactions, the sample was isothermally analyzed for 1 h at 900 °C, showing no evidences of further thermal events.

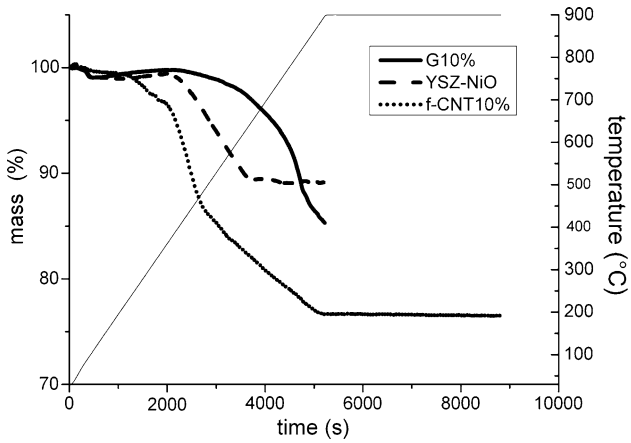

Fig. 4 Thermogravimetric curves of YSZ–NiO, YSZ–NiO + 10 mass% G and YSZ–NiO + 10 mass% f-CNT in 96%Ar/4%H_2

Several mechanisms have been proposed to explain the interaction of two solids, metal oxide and carbon, at temperatures in the 800–1000 °C range [8]. Considering the nickel carbothermal reduction in inert atmosphere, a possible mechanism is the one that considers the combination of the following reactions:

$$NiO(s) \rightarrow Ni(s) + 1/2\ O_2(g) \quad (1)$$

$$C(s) + O_2(g) \rightarrow CO_2(g) \quad (2)$$

At high oxygen partial pressure (pO_2) the equilibrium of the reaction (1) turns to the reactants, while reaction (2) processes towards the product, and the total consumption of the carbonaceous specie is observed with no nickel formed. On the other hand, under low pO_2 atmosphere the carbothermal reduction of NiO is favored, as long as carbon is available.

As YSZ is an oxygen ion conductor, with high mobility of O^{-2} ions, the influence of the ceramic phase matrix in the carbothermal reduction of NiO in argon was further studied by using both insulating Al_2O_3 and oxygen free SiC as ceramic matrixes in composites with 10 mass% of f-CNT. In addition, a TG analysis was performed for YSZ–CNT + 10%f-CNT with a previous Ar purge for 2 h at 30 °C. In the TG curves (Fig. 5), it can be seen that the nickel reoxidation occurred for all composites irrespectively of both the ceramic matrix and the Ar purge. These results indicate that residual oxygen in the measuring system is responsible for the reoxidation at high temperature under Ar flow. In fact, according to the Ellinghann diagrams the oxidation reaction is thermodynamically predicted even for

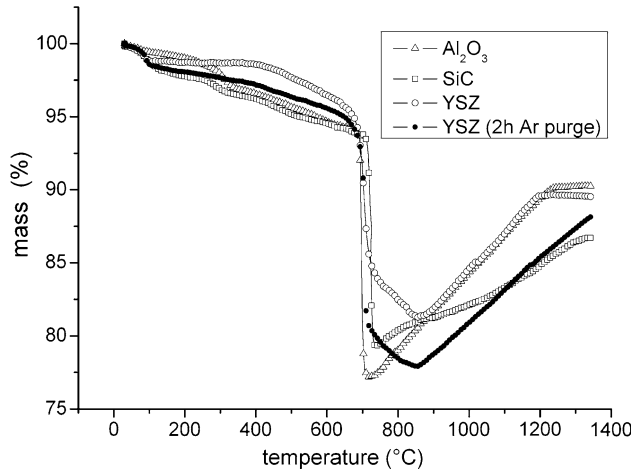

Fig. 5 Thermogravimetric curves of Al_2O_3–NiO 10 mass% f-CNT, SiC–NiO + 10 mass% f-CNT, YSZ–NiO + 10 mass% f-CNT in argon and of YSZ–NiO + 10 mass% f-CNT after 2 h argon purge at 30 °C

oxygen partial pressures lower than the ones expected for such a experimental conditions ($pO_2 \sim 10^{-6}$ atm) [9]. At high temperature the remaining carbon is no longer able to promote the carbothermal reduction reaction whereas the oxidation of the metal is kinetically favored.

Conclusions

The carbothermal reduction of nickel oxide in the composite YSZ–NiO is strongly dependent on the atmosphere, the amount of added carbon and the properties of the carbon material. In synthetic air the carbonaceous species were totally consumed without metal reduction. Thermogravimetric curves, measured under both inert and reducing atmosphere, suggest that the observed mass loss steps are associated with NiO reduction and oxidation of the excess of carbonaceous species. Such results were further supported by X-ray diffraction analyses. However, the observed reactions were also found to occur at different temperatures depending on the carbon material, and the more reactive functionalized carbon nanotubes display the lowest temperatures of maximum mass loss. The reoxidation of Ni at higher temperature was attributed to residual oxygen in the experimental apparatus. The present study revealed that carbothermal reduction of NiO may play an important role during the sintering of the composite. The study of the thermal evolution during heat treatment is important for the preparation of optimized microstructures of the solid oxide fuel cell anode.

Acknowledgements Authors are thankful to CNEN, CNPq (554970/2006-6, 555173/2005-4), and FINEP. Carbon nanotubes were produced at the Laboratório de Nanomaterias in the Physics Department of UFMG.

References

1. Minh NQ. Ceramic fuel cells. J Am Ceram Soc. 1993;76:563–88.
2. Muccillo R, Muccillo ENS, Fonseca FC, de Florio DZ. Characteristics and performance of electrolyte-supported solid oxide fuel cells under ethanol and hydrogen. J Electrochem Soc. 2008;155:B232–35.
3. de Florio DZ, Varela JA, Fonseca FC, Muccillo ENS, Muccillo R. Direcionamentos da tecnologia industrial de células a combustível de óxidos sólidos. Quim Nova. 2007;30:1339–46.
4. Singhal CS. Advances in solid oxide fuel cell technology. Solid State Ionics. 2000;135:305–13.
5. Trigueiro JPC, Silva GG, Lavall RL, Furtado CA, Oliveira S, Ferlauto AS, et al. Purity evaluation of carbon nanotube materials by thermogravimetric, TEM,and SEM methods. J Nanosci Nanotechnol. 2007;7:3477–86.
6. Li H, Zhao N, He C, Shi C, Du X, Li J. Thermogravimetric analysis and TEM characterization of the oxidation and defect sites of carbon nanotubes synthesized by CVD of methane. Mater Sci Eng. 2008;473:355–9.
7. Blachnio M, Staszczuk P, Grodzicka G. Adsorption and porosity properties of pure and modified carbon nanotube surface. J Therm Anal Calorim. 2008;94:641–8.
8. L′vov BV. Mechanism of carbothermal reduction of iron, cobalt, nickel and copper oxides. Thermochim Acta. 2000;360:109–20.
9. Richardson FD, Jeffes JE. The thermodynamics of substance of interest in iron and steelmaking from 0 to 2400 °C. I. Oxides. J Iron Steel Inst. 1948;160:261–70.